

Chapter 1

The Raw Material of Cluster Formation: Observational Constraints

Cathie J. Clarke

Star clusters form from reservoirs of dense cold gas ('Giant Molecular Clouds', henceforth GMCs) and in the following chapters we explore the wealth of recent simulations that follow this process, together with simulations that model the later (essentially gas-free) evolution of clusters.

A first step in any simulation is to decide on the initial conditions and for the cluster formation problem we need to specify the properties of GMCs (their typical densities and temperatures, levels of internal motions, homogeneity, etc.). We will mainly base these parameter choices on observational data and hence this chapter provides an overview of GMCs' observed properties. We will also use insights from larger scale (galaxy-wide) calculations in which GMCs emerge from simulations of the large scale interstellar medium (henceforth ISM). This brief overview is angled towards the kinds of issues that are relevant to understanding cluster formation and is no substitute for the kind of broader review of molecular clouds that can be found elsewhere: see for example Blitz (1991), Williams et al. (2000), McKee and Ostriker (2007), Fukui and Kawamura (2010), and Tan et al. (2013).

1.1 Overview of Molecular Cloud Observations

The total inventory of molecular gas in the Galaxy is estimated to be around $2.5 \times 10^9 M_{\odot}$, with about a third of the gas mass inward of the solar circle believed to be in molecular form (Wolfire et al. 2003); this number is somewhat uncertain because of the difficulty in detecting a possibly significant component in very cold gas (Loinard and Allen 1998). It is well known that molecular clouds are associated with spiral arms, both in the Milky Way (Heyer et al. 1998; Stark and Lee 2006) and in external galaxies (Helfer et al. 2003). This association is to be expected since spiral arms are

C.J. Clarke (✉)
Institute for Astronomy, University of Cambridge, Cambridge, UK
e-mail: cclarke@ast.cam.ac.uk

conspicuous in the blue light associated with young stars; since these stars have not had time to migrate far from their birth locations one would expect their natal gas to trace a similar pattern. The origin of the spiral pattern in the gas is believed to be the formation of shocks as the gas flow responds to the spiral pattern in the underlying mass distribution (Roberts 1969).

Stars form from molecular gas because the associated *Jeans mass* is low. The Jeans mass is the minimum mass required for gravitational collapse against support by pressure gradients and is given by:

$$M_J = 0.2 M_\odot \left(\frac{T_{10}^3}{n_5} \right)^{1/2}, \quad (1.1)$$

where T_{10} is the temperature in units of 10 K and n_5 is the number density of hydrogen normalised to 10^5 cm^{-3} (which is typical of the densest regions within GMCs). The corresponding length scale (r_J) is obtained by equating M_J with the mass contained within a sphere of radius r_J so that we obtain:

$$r_J = 0.06 \text{ pc} \left(\frac{T_{10}}{n_5} \right)^{1/2}. \quad (1.2)$$

A simple heuristic way of arriving at these scales is obtained by equating the timescales for free-fall collapse with the sound crossing timescale across a region. It is then unsurprising that cold and dense conditions (as found in GMCs) are associated with a low Jeans mass and a tendency towards gravitational collapse on small scales.

It is hard to assign meaningful ‘average’ properties to molecular clouds because of the hierarchical organisation of the ISM, consisting of nested structures on a large dynamic range of scales (see e.g. Scalo 1990; Elmegreen 2002). A plethora of terminology is used to describe local over-densities in terms of ‘clumps’ or ‘cores’ (Williams et al. 2000; Bergin and Tafalla 2007). We will discuss methods of characterising this hierarchy in Chap. 3 but for now there are a few numbers that are worth noting: molecular gas is organised into GMCs with typical masses in the range of a few $\times 10^5 M_\odot$ (these often being surrounded by atomic envelopes of similar mass; Blitz 1991). The mass distribution of GMCs is describable as a power-law with index -1.6 (Blitz et al. 2007), i.e. the fraction of clouds by number in a given mass range scales with cloud mass, M_{cl} , as $M_{\text{cl}}^{-1.6}$. This distribution is shallower (more mass on large scales) than the corresponding distribution for massive stars where the power-law index is -2.35 (Salpeter 1955). In the case of GMCs the power-law is however only defined over about an order of magnitude in mass since the largest GMCs in the Milky Way have masses slightly in excess of $10^6 M_\odot$ and the distribution is limited by completeness at the low mass end.

The mean column densities and mean volume densities of molecular clouds are of particular interest, being a little less than $\sim 10^{22} \text{ cm}^{-2}$ and $\sim 300 \text{ cm}^{-3}$ respectively. We discuss below how the former quantity depends on how the cloud boundary is defined (see Lombardi et al. 2010). The typical column density is at least partly set by the requirement that clouds are dense enough to be self-shielded against

photodissociation by the Galaxy’s ambient ultraviolet radiation field (van Dishoeck and Black 1988). The mean density $\bar{\rho}$ (which does not necessarily relate to a typical density of structures within clouds, given their clumpy structure, but is simply derived from the ratio of total mass to total volume) can be used to estimate a characteristic free-fall timescale through $t_{\text{ff}} \sim (G\bar{\rho})^{-1/2}$: this turns out to be about a Myr. This number will be relevant to our later discussions about whether GMCs collapse and form stars on a free-fall timescale.

Before proceeding further with a description of the empirical ‘laws’ that are applied to the internal structure of GMCs we now set out a brief guide to the techniques that are used to measure the properties of molecular clouds.

1.2 Observational Techniques Applied to GMCs

GMCs are predominantly composed of molecular hydrogen: it is therefore highly inconvenient that this molecule has no permanent dipole moment since this limits the transitions corresponding to observable lines. Indeed the lowest pure rotational level of H_2 has an excitation temperature of 510 K, which is far higher than the temperatures of molecular clouds (typically 10s of K away from regions of massive star formation). This problem has led to a number of other diagnostics being used as a *proxy* for H_2 . Below we summarise the complementary information that can be gleaned from line emission, dust emission and dust absorption, and discuss the advantages and disadvantages of each technique.

1.2.1 Molecular Line Emission

Line emission from a variety of abundant molecules is used to study cloud structure and kinematics. Early surveys (Solomon et al. 1987) used the second most abundant molecule in GMCs (^{12}CO); molecular clouds are generally optically thick in this emission so that it does not provide a good measure of cloud *mass*. It is thus preferable to use lower abundance molecules that are optically thin up to higher overall column densities. One of the most commonly used tracers is ^{13}CO (see Heyer et al. 2009); other commonly used molecules instead trace the densest gas within molecular clouds (e.g. NH_3 : Bergin and Tafalla 2007; Juvela et al. 2012; HCN: Gao and Solomon 2004; Wu et al. 2005 and CS: Plume et al. 1997; Shirley et al. 2003).

The most obvious benefit of using molecular line data in the present context is that it provides a unique diagnostic of cloud *kinematics* via Doppler shifted emission. It thus allows a determination of the dynamical state of GMCs and this will turn out to be very important information for initialising cluster formation simulations. Moreover, the use of transitions with different critical densities (i.e. densities at which collisional and radiative de-excitation rates are equal) provides information on *volume* densities, whereas dust emission/absorption only measures column densities. Finally, for those

with an interest in the chemistry of molecular clouds, molecular emission spectra provide important diagnostic information (see the reviews of Bergin and Tafalla 2007; Caselli and Ceccarelli 2012), constraining for example the free electron abundance (e.g. Bergin et al. 1999; Caselli et al. 2002) and the ages of star-forming regions (Doty et al. 2006).

On the other hand, chemical considerations can be a complicating factor when it comes to deriving the column density of H_2 from the flux in a given spectral line. There is a considerable debate in the literature about whether one can use a global conversion factor between CO and H_2 (Solomon et al. 1997; Blitz et al. 2007; Tacconi et al. 2008; Liszt et al. 2010; Wolfire et al. 2010; Sandstrom et al. 2013); additionally at high densities there is the issue of depletion of molecular gas on to grains (Redman et al. 2002; Jørgensen et al. 2005) so that gas phase diagnostics do not necessarily relate straightforwardly to the total abundance levels.

1.2.2 Dust Emission

Another widely used diagnostic of molecular cloud structure is thermal emission from dust. In order to derive the column density of gas from the flux density of dust emission at a single wavelength (usually in the millimetre or sub-millimetre range) one needs to be confident in a number of assumptions. One needs to know the fractional abundance of dust grains (compared with hydrogen), the dust emissivity law and the temperature of the emitting material. In practice one does not usually know the temperature *a priori* and thus multi-wavelength data is used to constrain this. Mapping with the *Herschel* Far Infrared satellite at wavelengths of 70–500 μm has recently provided dust continuum measurements at shorter wavelengths and has proved valuable for improving temperature constraints (e.g. Könyves et al. 2010).

The great advantage of thermal dust emission measurements is that they can not only be used to survey entire clouds—since even relatively dense structures in molecular clouds are still optically thin at millimetre wavelengths—they also allow the mapping of the densest regions of GMCs known as ‘dense cores’ (e.g. Motte et al. 1998; Johnstone et al. 2000). The disadvantages (apart from the lack of kinematic information) relate to uncertainties in the relationship between dust emissivity and gas mass (deriving both from uncertainties in dust emission properties and the dust to gas ratio). Moreover, in the case where a telescope beam contains emission components at a range of temperatures the mapping between multiwavelength dust emission and the total dust column can be under-constrained by the data.

1.2.3 Dust Absorption

This last difficulty is circumvented in the case of dust absorption measurements. This is because the attenuation of background sources by intervening dust depends

only on the dust opacity and absorption coefficients and not on the dust temperature. ‘Extinction mapping’ (e.g. Lombardi and Alves 2001; Lombardi et al. 2006) is based on measuring spatial variations in the distribution of infrared colours of background stars. By comparing this distribution with that in control fields ‘off-cloud’ such measurements can be used to deduce a column density map of the cloud (again with the above provisos about uncertainties in the dust opacities and dust to gas ratio). Deep near-infrared measurements mean that it is possible to penetrate large limiting column densities ($\sim 10^{23} \text{ cm}^{-2}$; Román-Zúñiga et al. 2010) and thus allow the mapping of dense cores; deep observations also improve the spatial resolution since they allow a denser sampling of the background stellar sources. Detailed comparison of maps obtained via continuum emission and via extinction mapping indicates fair agreement over all though with some differences (Bianchi et al. 2003; Goodman et al. 2009; Malinen et al. 2012).

1.3 Magnetic Support and the Star Formation Efficiency Problem

Following this summary of observational methods for measuring cloud masses and kinematics, we now consider the energy budget within clouds. It is well-established that the gravitational, kinetic and magnetic energies of GMCs are comparable in magnitude whereas their thermal energy is orders of magnitude smaller. (See below for a description of magnetic field measurements in molecular clouds). This hierarchy of energies immediately implies that GMCs are not (in contrast to stars) supported by thermal pressure and this has led to the view that clouds are supported by either turbulent motions or magnetic fields. There is however a problem with sustaining such support. As we have noted, clouds are highly clumped and since the kinetic energy densities are much higher than thermal energies this means that these clumps are in a state of highly supersonic motion. Collisions between clumps are expected to be highly dissipative and this should lead clouds to collapse on a free-fall time. At one time it was believed that this situation would be mitigated by magnetic fields (even if these fields were themselves insufficient to support a static cloud) since shocks are less dissipative if they are magnetically cushioned by fields in the plane of the shock. However, simulations of hydrodynamical and magneto-hydrodynamical (MHD) turbulence (Gammie and Ostriker 1996; Mac Low et al. 1998) demonstrated that magnetic fields do *not* increase the turbulent dissipation timescale (an effect that can be broadly understood from the fact that in a turbulent medium the fields are not always parallel to shock fronts).

On the other hand, magnetic fields of sufficient strength *can* impede cloud collapse even in the absence of internal cloud motions. The ability of magnetic fields to support a static cloud against gravitational collapse can be cast in terms of a critical mass-to-flux ratio (Mouschovias and Spitzer 1976). We can derive a heuristic estimate for this value (by analogy with our description of the Jeans mass above) by

comparing the free-fall collapse time with the timescale for Alfvén wave propagation: Alfvén waves propagate through a magnetised medium at a speed of $(B^2/\mu_0\rho)^{1/2}$ (for magnetic flux density B , magnetic permeability μ_0 and density ρ) and represent an important dynamical communication mode in magnetised media. The result of this exercise is that the critical mass-to-flux ratio is simply given by a factor of order unity times $G^{-1/2}$. Note that the critical Jeans mass (see Eq. 1.1) depends on gas density and therefore this changes—if the initial mass exceeds the initial Jeans mass—as a cloud collapses; for magnetised clouds the critical mass-to-flux ratio is however constant. Thus—provided that the magnetic field remains ‘frozen’ to the gas (i.e. the mass-to-flux ratio is fixed)—the ratio of a cloud’s mass-to-flux ratio to the critical value is itself constant. The extent to which a cloud is either subcritical or supercritical thus does not change during collapse. It was at one time widely assumed that magnetic fields are indeed sub-critical and thus non-ideal MHD effects (specifically ambipolar diffusion: Mestel and Spitzer 1956; Galli and Shu 1993; McKee et al. 1993) were invoked as a means to slowly increase the mass-to-flux ratio and hence modulate the rate of cloud collapse (and star formation).

Subsequently there has been considerable observational effort devoted to the measurement of magnetic fields in star-forming clouds. Although the morphology of the magnetic field in the plane of the sky can be inferred from dust polarisation measurements (e.g. Heiles 2000), its magnitude can only be estimated through Zeeman polarimetry on Zeeman sensitive lines such as OH, CN and HI. Such measurements however only measure the component of the magnetic field along the line-of-sight and thus needs to be assessed in a statistical sense from a large ensemble of measurements. Early studies (Crutcher 1999) indicated that the mass-to-flux ratios in molecular clouds were close to critical (i.e. confirming that the magnetic energy density was of comparable magnitude to the gravitational potential energy). A decade of further observations and analysis has led to the conclusion that the mass-to-flux ratio is roughly twice critical: Crutcher et al. (2010) noted that the Zeeman data was ‘inconsistent with magnetic support against gravity’ and noted that the observed scaling of magnetic field strength with density ($B \propto \rho^{2/3}$) was as expected if the magnetic field was being passively advected in a gravitationally dominated flow. This situation is in contrast to that in the diffuse (atomic) interstellar medium where magnetic fields are instead sub-critical (Heiles and Troland 2004) and the lack of correlation between magnetic field strength and density is indicative of magnetically dominated conditions.

Clearly, therefore, magnetic fields must be important in the process of GMC formation from the diffuse medium (Kim and Ostriker 2006; Mouschovias et al. 2009). Even on the scale of GMC interiors (which will form the subject of much of these chapters), the only mildly super-critical conditions mean that magnetic fields should *not* be ignored. It is worth emphasising that most of the simulations described below omit magnetic fields for purely practical reasons.

The above results have an important implication for what is often described as the ‘star formation efficiency problem’. Given that hydrodynamical and MHD turbulence both dissipate on a free-fall time and given that magnetic fields are insufficient to

prevent collapse, we are left to conclude that clouds should collapse on a free-fall timescale, unless there are mechanisms that re-inject energy into the turbulence. We might therefore expect—unless the formation of stars itself disperses the remaining gas—that the timescale on which a GMC is converted into stars is its free-fall time (~ 1 Myr). There are however a number of observational indications that this is *not* the case. If we divide the entire mass of molecular gas in the Milky Way ($\sim 10^9 M_\odot$) by a typical cloud free-fall timescale, we would expect that the Galactic star formation rate would be $\sim 10^3 M_\odot \text{ yr}^{-1}$, which exceeds the observed rate by more than two orders of magnitude. We therefore conclude that the star formation rate associated with GMCs (averaged over the time that gas is within GMCs) is much less than the total mass in GMCs divided by the free-fall time.

This conclusion, based on galaxy-wide scales, has been confirmed by recent studies within individual GMCs. Probably the most comprehensive study to date is that of (Evans et al. 2009) which used the *Spitzer* ‘Cores to Disks’ Legacy Survey to compare the census of young stars with the magnitude of the available mass reservoir. The results of this exercise confirmed that star formation is indeed inefficient with around 3–6% of the cloud mass being converted into stars per free-fall time.

1.4 Scaling Relations

Following the first large-scale surveys of the structure and kinematics of molecular clouds, several correlations (‘scaling relations’) were noted by Larson (1981). These are now known widely as ‘Larson’s Laws’ and concern the inter-relationship between mass, linear size and velocity width for structures within molecular clouds:

1. The velocity dispersion σ across structures of different size (R) scales as $\sigma \propto R^{0.5}$ (see Solomon et al. 1987). Since this relation was derived from radio line observations it is often termed the ‘size linewidth’ relation: see Fig. 1.1.
2. The mass (M), R and σ are related by $M \sim R\sigma^2/G$.
3. The mean density varies inversely with R or (equivalently) different structures within clouds share a roughly constant column density: $M \propto R^2$. Note that a situation of constant column density cannot be true in detail or else there would be no contrast between different structures within clouds. Lombardi et al. (2010) have shown that extinction mapping (see Sect. 1.2.3) within several GMCs demonstrates that the distribution of column densities within a cloud is describable as a log normal. The mean column density within a cloud depends on the level at which the data is thresholded (i.e. what is the lower limit on extinction used to define the cloud boundary). Since the distribution of column densities appears to be rather similar from cloud to cloud, the mean column density is indeed similar in different clouds, provided the clouds are analysed above the same extinction contour.

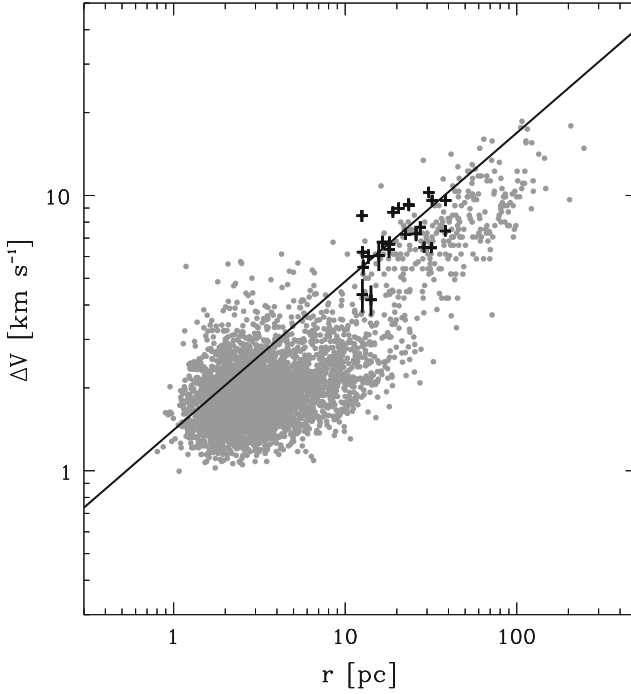


Fig. 1.1 Size-line width radius relationship for molecular clouds in M33 (*crosses*). The *grey dots* represent Milky Way molecular cloud data from Solomon et al. (1987) and Heyer et al. (2001). The power-law fit gives $\Delta V \propto r^{0.45 \pm 0.02}$. Figure from Rosolowsky et al. (2003)

It can immediately be seen that any two of Larson’s laws imply the third and so one would like to know which two of the laws are ‘fundamental’ and which one is just a consequence of the other two. We will consider (1) and (2) in a little more detail.

It is often said that molecular clouds exhibit supersonic turbulence: supersonic motions are of course immediately implied by the high ratio of kinetic to thermal energy in GMCs that was noted in Sect. 1.3. It is debatable whether these strong internal motions can strictly be described as turbulence (where this is understood to represent a *steady state* cascade of energy from a large [driving] scale to the small scale at which it is dissipated). Larson however pointed out that the first law was roughly consistent with such a scenario. If one considers a power spectrum $P(k) \propto k^{-a}$ (where k is related to the wavelength, λ via $k = 2\pi/\lambda$) then the kinetic energy per unit mass associated with wave vectors in the range k , to $k + dk$ is given by $P(k)k^2dk$. From this one can deduce that the mean square velocity associated with size scale R should scale as $\sigma^2 \propto R^{(a-3)}$ and thus the Larson Law would suggest a power spectrum with $a = 4$. This value is suggestively close to several well-studied categories of turbulence (e.g. incompressible ‘Kolmogorov’ turbulence has $a = 11/3$, compressible ‘Burgers’ turbulence has $a = 4$ while MHD turbulence

has $a = 3.5$). Myers and Gammie (1999) explored this possibility further, examining the case of injection at finite driving scales. They pointed out that the asymptotic relationships described above should flatten out at size scales above the ‘driving’ scale: the fact that this is *not* observed within GMCs (see Fig. 1.1) then implies that the driving scale is large (of order 100 pc or above), and would suggest that energy is injected into the clouds from the larger scale galactic environment.

A large body of work has been devoted to modelling GMCs as turbulent systems but it is worth repeating that we do not know whether GMCs have had time to achieve the steady state turbulent cascade that is observed in situations of laboratory turbulence. If they are indeed in such a steady state, then the turbulent structure depends only on the physical conditions in the medium (compressibility, presence of magnetic fields, etc.) and not on the initial conditions. If they are not in a steady state (as is the case for a large category of the simulations that we will discuss in forthcoming chapters, where clouds fragment into stars on a free-fall time) then the statistics describing kinematic and density structures are constantly evolving. In this case the power spectrum partly reflects the formation history of the cloud and it becomes particularly important to understand the nature of the relationship between the internal kinematics of GMCs and their interaction with the wider environment.

Turning now to Larson’s second law, we note that there are several different interpretations. One extreme interpretation would be to say that Larson’s 1st and 3rd laws are ‘fundamental’ for some reason and that therefore the 2nd law ($\sigma^2 \propto M/R$) is just a mathematical consequence of the other two laws. In this extreme interpretation, this scaling has nothing to do with the role of gravity in molecular clouds. Another interpretation is to note that the constant of proportionality in this relation is of order G (the gravitational constant), suggesting that self-gravity plays an important role in determining cloud structure. Note that this is a weaker statement than another extreme version which maintains that clouds are in a state of virial equilibrium (which has led to this assumption being used in order to *determine* cloud masses, e.g. Blitz et al. 2007; Bolatto et al. 2008).

Much observational data has been assembled on the masses and kinematics of a range of clouds, both in the Galaxy (Heyer et al. 2009) and in extragalactic environments (Rosolowsky 2007; Bolatto et al. 2008). These studies express the degree of gravitational boundedness of clouds in terms of a parameter α_{vir} which is proportional to the ratio of kinetic energy to potential energy and which would be unity in the case of a spherical cloud in virial equilibrium (and equal to 2 in the case of a marginally unbound spherical cloud). A large scatter in α_{vir} values is found at all masses, with values ranging from somewhat less than 1 to around 10 (see Fig. 1.2). It is not clear what fraction of this scatter can be attributed to observational uncertainties. The mean is close enough to unity to discourage the idea that gravity is irrelevant to this relation. Nevertheless the large scatter means that it is still arguable whether the bulk of clouds are gravitationally bound or unbound; as we shall see later (see Chap. 4, Fig. 4.1), rather small differences in α_{vir} in the region of marginal boundedness can have dramatic effects on the star formation rate.

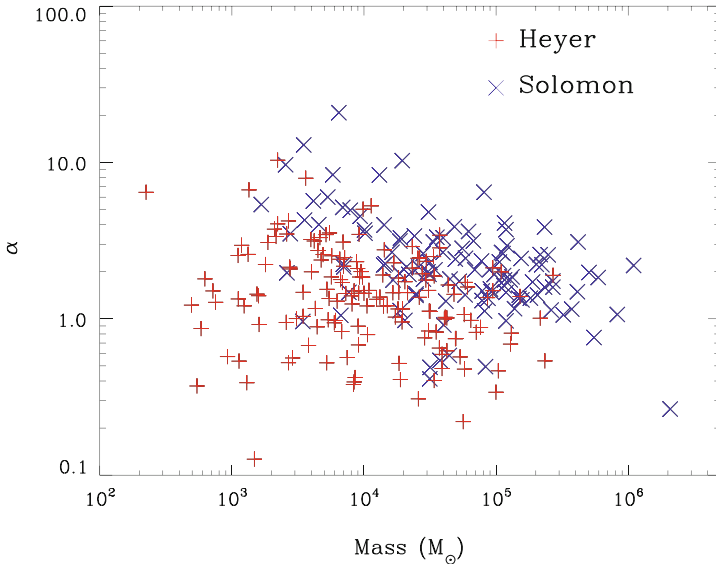


Fig. 1.2 Plot of the gravitational parameter (α ; see text) as a function of molecular cloud mass from Solomon et al. (1987) and Heyer et al. (2009). Figure from Dobbs et al. (2011b)

1.5 GMCs and the Large-Scale ISM

At this point we can start to see that the properties of GMCs are quite well characterised observationally but that we do not understand some important empirical facts (such as why the fraction of clouds that is converted into stars per crossing time is so low, nor what drives the inter-relationship between the Larson scaling relations). In both cases it is likely that the answers are related to processes that originate beyond the GMCs themselves in the wider galactic environment.

In recent years, advances in computational power have enabled some ambitious galaxy-wide simulations that have started to shed some light on the relationship between GMCs and the wider ISM: for example, the grid based calculations of Tasker and Tan (2009) and the complementary smoothed particle hydrodynamics (SPH) calculations of Dobbs et al. (2011a). From the perspective of our present discussion, the main questions of interest are whether such galaxy-wide simulations give rise to GMC-like structures that, for example, obey the scaling relations discussed above (it should be stressed that the ‘clouds’ formed in this simulation are in themselves insufficiently resolved for one to follow star formation within them directly). It is found that the simulations do a reasonable job at reproducing the size-line width relation, although the dynamic range of the simulated clouds is small compared with that covered by observations. It is however hard to identify exactly what physical processes contribute to the form of the relationship in the simulated clouds (indeed

Dobbs and Bonnell 2007 have shown that such a relationship is readily obtained from a variety of situations where clouds form in clumpy shocks, even in the absence of self-gravity).

The kinetic and potential energy contents of clouds formed in galaxy-wide simulations have also been analysed and demonstrate that a number of factors (including numerical resolution; Tasker and Tan 2009) affect whether clouds are predominantly bound or unbound. For example, Dobbs et al. (2011a) found that clouds were predominantly unbound in the case of magnetised simulations on account of the role of magnetic fields in inhibiting collapse. In the absence of magnetic fields or (parametrised) supernova feedback, cloud collapse produces a roughly virialised (hence bound) state; however even in the absence of magnetic fields the number of unbound clouds increases strongly as the strength of the feedback is increased. Dobbs et al. (2011a) argued that the latter is more realistic since the unbound clouds in the simulation are rather aspherical (similar to those observed; Koda et al. 2006) whereas gravitationally bound clouds collapse to more spherical configurations.

A further cloud diagnostic that may relate to the mode of cloud assembly is whether the net cloud rotation is prograde or retrograde (with respect to the rotation of the host galaxy). Rosolowsky et al. (2003) noted that a surprisingly large number of clouds in M33 were counter-rotating and that the magnitude of rotation in the prograde population was too small to be consistent with angular momentum conserving collapse associated with gravitational instability. The simulations of Dobbs (2008) suggested that those (generally higher mass) clouds that are self-gravitating are indeed prograde, but that an important population of smaller clouds, which are formed mainly by agglomeration, display a mixture of prograde and retrograde spin directions.

A final point to emerge from these larger scale simulations is that they agree on the importance of encounters between clouds. This is a caveat that should be borne in mind when interpreting the simulations that we will be discussing later, which (for reasons of computational economy) consider cloud evolution *in isolation*. For example, Tasker and Tan (2009) emphasise that their cloud-cloud collision timescales are shorter than many estimates of GMC lifetimes and that ‘...an individual GMC is just as likely to have its properties dramatically altered by a merger than by a destructive mechanism such as supernova feedback or ionization feedback’. In a similar vein, Dobbs et al. (2011a) note that ‘...the constituent gas in GMCs is likely to change on timescales of Myr... A cloud seen after 30 Myr may not be a counterpart to any cloud present at the current time’.

Evidently such large-scale simulations are in their infancy and at this stage some of the insights are rather qualitative. It however appears ‘rather easy’ to produce clouds whose properties (mass, spins, morphology, internal kinematics, gravitational energy) roughly match those observed. In the simulations, both self-gravity and agglomeration play roles in cloud creation, with the former being increasingly important at larger cloud scales. Moreover, the simulations raise important doubts about the legitimacy of treating any GMC’s evolution as being truly isolated from its environment and paint a picture in which clouds’ individual identities are mutable on timescales of Myr.

1.6 Summary: Key Observational Constraints for Simulations

We will proceed in the following chapters to describe a variety of hydrodynamical simulations of star and cluster formation and so we end this chapter by listing the key factors that should inform the design and interpretation of such simulations: (i) It is necessary to model loosely bound and unbound clouds. (ii) Ideally such simulations should include magnetic fields, since the magnetic energy density in clouds is similar in magnitude to their kinetic and gravitational energies. (iii) Ideally such simulations should model interaction with the surroundings—this is particularly hard to model in a meaningful way without resorting to galaxy-scale simulations and thus sacrificing resolution within clouds. (iv) Clouds should not necessarily be regarded as examples of fully developed (steady state) turbulence, especially given the insights above about the transient lifetimes of clouds as distinct entities. (v) Finally, the results of such simulations need to be monitored with regard to the ‘efficiency’ (rate per free-fall time) of their resulting star formation, in order that they do not exceed the upper limits imposed by observations.

References

- Bergin, E. A. & Tafalla, M. 2007, *ARA&A*, 45, 339
- Bergin, E. A., Plume, R., Williams, J. P., & Myers, P. C. 1999, *ApJ*, 512, 724
- Bianchi, S., Gonçalves, J., Albrecht, M., et al. 2003, *A&A*, 399, L43
- Blitz, L. 1991, in *NATO ASIC Proc. 342: The Physics of Star Formation and Early Stellar Evolution*, ed. C. J. Lada & N. D. Kylafis, 3
- Blitz, L., Fukui, Y., Kawamura, A., et al. 2007, in *Protostars and Planets V*, ed. B. Reipurth, D. Jewitt & K. Kell, University of Arizona Press, 81
- Bolatto, A. D., Leroy, A. K., Rosolowsky, E., Walter, F., & Blitz, L. 2008, *ApJ*, 686, 948
- Caselli, P. & Ceccarelli, C. 2012, *A&A Rev.*, 20, 56
- Caselli, P., Walmsley, C. M., Zucconi, A., et al. 2002, *ApJ*, 565, 331
- Crutcher, R. M. 1999, *ApJ*, 520, 706
- Crutcher, R. M., Wandelt, B., Heiles, C., Falgarone, E., & Troland, T. H. 2010, *ApJ*, 725, 466
- Dobbs, C. L. 2008, *MNRAS*, 391, 844
- Dobbs, C. L. & Bonnell, I. A. 2007, *MNRAS*, 374, 1115
- Dobbs, C. L., Burkert, A., & Pringle, J. E. 2011a, *MNRAS*, 417, 1318
- Dobbs, C. L., Burkert, A., & Pringle, J. E. 2011b, *MNRAS*, 413, 2935
- Doty, S. D., van Dishoeck, E. F., & Tan, J. C. 2006, *A&A*, 454, L5
- Elmegreen, B. G. 2002, *ApJ*, 564, 773
- Enoch, M. L., Glenn, J., Evans, II, N. J., et al. 2007, *ApJ*, 666, 982
- Evans, II, N. J., Dunham, M. M., Jørgensen, J. K., et al. 2009, *ApJS*, 181, 321
- Fukui, Y. & Kawamura, A. 2010, *ARA&A*, 48, 547
- Galli, D. & Shu, F. H. 1993, *ApJ*, 417, 220
- Gammie, C. F. & Ostriker, E. C. 1996, *ApJ*, 466, 814
- Gao, Y. & Solomon, P. M. 2004, *ApJS*, 152, 63
- Goodman, A. A., Pineda, J. E., & Schnee, S. L. 2009, *ApJ*, 692, 91
- Hatchell, J., Richer, J. S., Fuller, G. A., et al. 2005, *A&A*, 440, 151
- Heiles, C. 2000, *AJ*, 119, 923
- Heiles, C. & Troland, T. H. 2004, *ApJS*, 151, 271
- Helfer, T. T., Thornley, M. D., Regan, M. W., et al. 2003, *ApJS*, 145, 259
- Heyer, M. H., Brunt, C., Snell, R. L., et al. 1998, *ApJS*, 115, 241

- Heyer, M. H., Carpenter, J. M., & Snell, R. L. 2001, *ApJ*, 551, 852
- Heyer, M. H., Krawczyk, C., Duval, J., & Jackson, J. M. 2009, *ApJ*, 699, 1092
- Johnstone, D., Wilson, C. D., Moriarty-Schieven, G., et al. 2000, *ApJ*, 545, 327
- Johnstone, D., Di Francesco, J., & Kirk, H. 2004, *ApJ*, 611, L45
- Jørgensen, J. K., Schöier, F. L., & van Dishoeck, E. F. 2005, *A&A*, 437, 501
- Juvela, M., Harju, J., Ysard, N., & Lunttila, T. 2012, *A&A*, 538, 133
- Kim, W.-T. & Ostriker, E. C. 2006, *ApJ*, 646, 213
- Koda, J., Sawada, T., Hasegawa, T., & Scoville, N. Z. 2006, *ApJ*, 638, 191
- Könyves, V., André, P., Men'shchikov, A., et al. 2010, *A&A*, 518, L106
- Larson, R. B. 1981, *MNRAS*, 194, 809
- Liszt, H. S., Pety, J., & Lucas, R. 2010, *A&A*, 518, 45
- Loinard, L. & Allen, R. J. 1998, *ApJ*, 499, 227
- Lombardi, M. & Alves, J. 2001, *A&A*, 377, 1023
- Lombardi, M., Alves, J., & Lada, C. J. 2006, *A&A*, 454, 781
- Lombardi, M., Alves, J., & Lada, C. J. 2010, *A&A*, 519, L7
- Mac Low, M.-M., Klessen, R. S., Burkert, A., & Smith, M. D. 1998, *Physical Review Letters*, 80, 2754
- Malinen, J., Juvela, M., Rawlings, M. G., et al. 2012, *A&A*, 544, 50
- McKee, C. F. & Ostriker, E. C. 2007, *ARA&A*, 45, 565
- McKee, C. F., Zweibel, E. G., Goodman, A. A., & Heiles, C. 1993, *Protostars and Planets III*, ed. E. H. Levy & J. I. Lunine, University of Arizona Press, 327
- Mestel, L. & Spitzer, Jr., L. 1956, *MNRAS*, 116, 503
- Motte, F., André, P., & Neri, R. 1998, *A&A*, 336, 150
- Mouschovias, T. C. & Spitzer, Jr., L. 1976, *ApJ*, 210, 326
- Mouschovias, T. C., Kunz, M. W., & Christie, D. A. 2009, *MNRAS*, 397, 14
- Myers, P. C. & Gammie, C. F. 1999, *ApJ*, 522, L141
- Plume, R., Jaffe, D. T., Evans, II, N. J., Martín-Pintado, J., & Gómez-González, J. 1997, *ApJ*, 476, 730
- Redman, M. P., Rawlings, J. M. C., Nutter, D. J., Ward-Thompson, D., & Williams, D. A. 2002, *MNRAS*, 337, L17
- Roberts, W. W. 1969, *ApJ*, 158, 123
- Román-Zúñiga, C. G., Alves, J. F., Lada, C. J., & Lombardi, M. 2010, *ApJ*, 725, 2232
- Rosolowsky, E. 2007, *ApJ*, 654, 240
- Rosolowsky, E., Engargiola, G., Plambeck, R., & Blitz, L. 2003, *ApJ*, 599, 258
- Salpeter, E. E. 1955, *ApJ*, 121, 161
- Sandstrom, K. M., Leroy, A. K., Walter, F., et al. 2013, *ApJ*, 777, 5
- Scalo, J. 1990, in *Astrophysics and Space Science Library*, Vol. 162, *Physical Processes in Fragmentation and Star Formation*, ed. R. Capuzzo-Dolcetta, C. Chiosi, & A. di Fazio, Kluwer Academic Publishers, 151
- Shirley, Y. L., Evans, II, N. J., Young, K. E., Knez, C., & Jaffe, D. T. 2003, *ApJS*, 149, 375
- Solomon, P. M., Rivolo, A. R., Barrett, J., & Yahil, A. 1987, *ApJ*, 319, 730
- Solomon, P. M., Downes, D., Radford, S. J. E., & Barrett, J. W. 1997, *ApJ*, 478, 144
- Stark, A. A. & Lee, Y. 2006, *ApJ*, 641, L113
- Tacconi, L. J., Genzel, R., Smail, I., et al. 2008, *ApJ*, 680, 246
- Tan, J. C., Shaske, S. N., & Van Loo, S. 2013, in *IAU Symposium*, Vol. 292, *Molecular Gas, Dust and Star Formation in Galaxies*, ed. T. Wong & J. Ott, Cambridge University Press, 19
- Tasker, E. J. & Tan, J. C. 2009, *ApJ*, 700, 358
- van Dishoeck, E. F. & Black, J. H. 1988, *ApJ*, 334, 771
- Williams, J. P., Blitz, L., & McKee, C. F. 2000, *Protostars and Planets IV*, ed. V. Manning, A. P. Boss & S. S. Russell, University of Arizona Press, 97
- Wolfire, M. G., McKee, C. F., Hollenbach, D., & Tielens, A. G. G. M. 2003, *ApJ*, 587, 278
- Wolfire, M. G., Hollenbach, D., & McKee, C. F. 2010, *ApJ*, 716, 1191
- Wu, J., Evans, II, N. J., Gao, Y., et al. 2005, *ApJ*, 635, L173